

Quasinormal modes of nonlinear electromagnetic black holes from unstable null geodesics.

N. Bretón¹ and L. A. López²

¹ *Dpto de Física, Centro de Investigación y de Estudios Avanzados del I.P.N., Apdo. 14-740, D.F., México. and*

² *Área Académica de Matemáticas y Física, UAEH, Carretera Pachuca-Tulancingo Km. 4.5, C. P. 42184, Pachuca, México.*

Abstract

The expressions for the quasinormal modes (QNMs) of black holes with nonlinear electrodynamics, calculated in the eikonal approximation, are presented. In the eikonal limit QNMs of black holes are determined by the parameters of the circular null geodesics. The unstable circular null orbits are derived from the effective metric that is the one obeyed by light rays under the influence of a nonlinear electromagnetic field. As an illustration we calculate the QNMs of four nonlinear electromagnetic black holes, two singular and two regular, namely from Euler-Heisenberg and Born-Infeld theories, for singular, and the magnetic Bardeen black hole and the one derived by Bronnikov for regular ones. Comparison is shown with the QNMs of the linear electromagnetic counterpart, their Reissner-Nordström black hole.

PACS numbers: 04.70.Bw,05.45.-a,41.20.Jb,42.15.-i

I. INTRODUCTION

When a black hole undergoes perturbations, the resulting behavior can be described in three stages. The first stage corresponds to radiation due to the initial conditions of the perturbations. The second stage corresponds to damped oscillations with complex frequencies. The third stage in general corresponds to a power law decay of the fields. The modes of such oscillations are called quasi-normal modes (QNMs). The frequencies of QNMs are independent of initial perturbations, they are then the intrinsic imprint of the response of the black hole to external perturbations.

Besides the importance of QNMs in the analysis of black hole stability, they play an outmost role in characterising gravitational wave signals, as the ones recently detected at LIGO, as well as the promised ones jointly with VIRGO collaboration and the planned space antenna project LISA [1]. QN resonances, being the characteristic “sound” of the black hole itself, are crucial to identify the spacetime parameters, especially the mass and angular momentum of the black hole, but as well are going to be important on identifying additional physical parameters arising from more realistic black hole models.

There are also theoretical reasons that justify the study of QNMs, one of them from Loop Quantum Gravity (LQG). It has been observed that for asymptotically flat black holes, the real part of the high overtones of QNMs coincide with the Barbero-Immirzi parameter [2]; this parameter measures the size of the quantum area in Planck units in relation to the counting of microstates in LQG.

Mashhoon [3] [4] has suggested an analytical technique of calculating the QNMs in the geometric-optics (eikonal) limit. The basic idea is to interpret the black-hole free oscillations in terms of null particles trapped at the unstable circular orbit and slowly leaking out. The real part of the complex quasinormal frequencies (QNFs) is determined by the angular velocity at the unstable null geodesic; the imaginary part is related to the instability time scale of the orbit. In such a way that QNMs can be determined from the unstable null geodesics that are the orbits attached to the maximum of the effective potential barrier felt by light rays on their interaction with the black hole. In this sense Cardoso [5] showed the relationship among unstable null geodesics, Lyapunov exponents and quasinormal modes in a stationary spherically symmetric space-time.

It is well known that in situations involving strong electromagnetic fields, the linear

superposition does not hold and nonlinear effects, for instance the creation of electron-positron pairs or scattering of light by light, are very likely to occur. These situations are described by Quantum Electrodynamics (QED); alternatively, classical theories that include these nonlinear phenomena in an effective way may be useful. Among these theories are the Euler-Heisenberg (EH) and the Born-Infeld (BI) [6]. Moreover, nonlinear electromagnetic (NLEM) theories have attracted attention lately due to their ability in suppressing the singularity in some black hole solutions. As a result of the nonlinear interaction, light rays do not follow the null geodesics of the background metric, but do follow the null geodesics of an effective metric that depends on the nonlinear electromagnetic energy momentum tensor [7] [8].

In [9] applying the ideas of Cardoso, were determined the QNMs of the regular magnetic black hole model proposed by Bardeen, which is a solution of nonlinear electrodynamics coupled to Einstein gravity. QNMs of nonlinear electromagnetic black holes were computed, using the WKB method, for the Born-Infeld black hole in [10] and for the Bronnikov black hole in [11]. Our study differs from previous ones in the fact that we use the effective metric to determine the unstable circular orbits followed by light rays. Otherwise the QNFs correspond to massless test particles, that indeed follow, in the eikonal approximation, the null geodesics of the background metric. Those QNFs do not correspond to light rays, that in the presence of strong electromagnetic fields do interact among themselves giving rise to nonlinear effects.

Using the effective metric and the corresponding effective potential we derive the Lyapunov exponent expression, that is related to the imaginary part of the quasinormal frequencies (QNF); as an illustration we address two examples of singular black holes: the Born-Infeld and a magnetic Euler-Heisenberg one, as well as two examples of regular black holes, the Bardeen model for a magnetic self-gravitating black hole and one solution derived by Bronnikov.

The paper is organized as follows: In Sect. II we give a brief explanation to determining the QNFs using the unstable null geodesics and the Lyapunov exponent. In Sect. III a short summary of the nonlinear electrodynamics for a static spherically symmetric spacetime is presented as well as the effective NLEM metric. In Sect. IV the expressions for the real and imaginary parts of the QNFs in terms of the NLEM Lagrangian are given. In Sect. V we analyze the QNFs of the four examples above mentioned. In each case the QNFs are

compared with the ones corresponding to the massless test particles and light rays of the Reissner-Nordstrom (RN) black hole. Conclusions are given in the last section.

II. QNM AND THE LYAPUNOV EXPONENT

The connection between the QNMs and bound states of the the inverted black hole effective potential was pointed out in [4]. In [5] it is shown that, in the eikonal limit, the QNMs of black holes in any dimensions are determined by the parameters of the circular null geodesics. The real part of the complex QNM frequencies is determined by the angular velocity at the unstable null geodesics. The imaginary part is related to the instability time scale of the orbit, and therefore related to the Lyapunov exponent that is its inverse. Lyapunov exponents are a measurement of the average rate at which nearby trajectories converge or diverge in the phase space. A positive Lyapunov exponent indicates a divergence between nearby trajectories, i.e., a high sensitivity to initial conditions. In the case of stationary, spherically symmetric spacetimes it turns out that this exponent can be expressed as the second derivative of the effective potential evaluated at the radius of the unstable circular null orbit. It was also shown the agreement of the so calculated QNMs with the analytic WKB approximation,

$$\omega_{QNM} = \Omega_c l - i(n + \frac{1}{2})|\lambda| \quad (1)$$

where n is the overtone number and l is the angular momentum of the perturbation. Ω_c is the angular velocity at the unstable null geodesic and λ is the Lyapunov exponent, determining the instability time scale of the orbit. From the equations of motion for a test particle in the static spherically symmetric (SSS) spacetime, $\dot{r}^2 = V_r$, where V_r is the effective potential for radial motion, circular geodesics are determined from the conditions $V(r_c) = V'(r_c) = 0$ where r_c is the radius of the circular orbit. The Lyapunov exponent in terms of the second derivative of the effective potential is given by

$$\lambda = \sqrt{\frac{V_r''}{2\dot{t}^2}}, \quad (2)$$

where t is the time coordinate. The dot denotes the derivative with respect to an affine parameter and the prime stands for the derivative with respect to r . The orbital angular velocity is given by

$$\Omega_c = \frac{d\varphi}{dt} = \frac{\dot{\varphi}}{\dot{t}}. \quad (3)$$

For our purpose both expressions should be evaluated at r_c , the radius of the unstable null circular orbit, that is the orbit with an impact parameter b_c related to the effective potential as $V_r = 1/b_c^2$, i. e. orbits with an energy equal to the maximum of the effective potential.

For a static spherically symmetric background

$$ds^2 = f(r)dt^2 - \frac{1}{g(r)}dr^2 - r^2d\Omega^2, \quad (4)$$

the energy E and the angular momentum L of a test particle are conserved quantities,

$$f(r)\dot{t} = -E = \text{const}, \quad r^2\dot{\varphi} = -L = \text{const}. \quad (5)$$

For equatorial orbits ($\theta = \pi/2$), the equation for radial motion is $\dot{r}^2 = V_r$. For the case of a static spacetime $f = g$ in (4), and the effective potential is given by

$$V_r = g(r) \left[\frac{E^2}{f(r)} - \frac{L^2}{r^2} \right] = E^2 - f \frac{L^2}{r^2}. \quad (6)$$

Then the Lyapunov exponent, related to the imaginary part of the QNF, from (2) is given by

$$\lambda^2 = \frac{f_c}{2r_c^2} \left[2f_c - r_c^2 f_c'' \right], \quad (7)$$

while the orbital angular velocity, that is proportional to the QNF real part, is given by

$$\Omega_c = \frac{L}{r_c^2} \frac{f_c}{E} = \sqrt{\frac{f_c}{r_c^2}}. \quad (8)$$

In the previous expressions (7) and (8) the conditions for a circular orbit, $V_r = 0$ and $V_r' = 0$ that amount, respectively, to

$$\frac{E^2}{L^2} = \frac{f}{r^2}, \quad \text{and} \quad 2f - r f' = 0, \quad (9)$$

have been incorporated.

In the following section (7) and (8) will be determined from the effective metric, and λ and Ω_c will be written in terms of the NLEM Lagrangian.

III. QNMS OF NLEM BLACK HOLES FROM THE EFFECTIVE METRIC

The action for gravitation coupled to an electromagnetic field is given by

$$S = \frac{1}{16\pi} \int d^4x \sqrt{-g} [R - L(F)], \quad (10)$$

where R is the scalar curvature and L is an arbitrary function of the electromagnetic invariant $F = F^{\mu\nu} F_{\mu\nu}$, with $F_{\mu\nu} = \partial_\mu A_\nu - \partial_\nu A_\mu$ being the electromagnetic field tensor. For the Maxwell theory the Lagrangian is directly proportional to F , $L_M = F$. We note that the most general Lagrangian can depend on both electromagnetic invariants, F and $G = \mathcal{F}^{\mu\nu} F_{\mu\nu}$, where $\mathcal{F}^{\mu\nu}$ is the dual field-strength electromagnetic tensor. In this work we shall restrict ourselves to lagrangians depending only on F but otherwise completely general. Roughly speaking this restriction has the consequence of having solutions with only electric or magnetic charges, but not both.

The electromagnetic tensor compatible with spherical symmetry has two nonzero components, $F_{01} = -F_{10}$ and $F_{23} = -F_{32}$, corresponding to the radial electric and magnetic fields, with

$$r^2 L_F F^{10} = q_e, \quad F_{23} = q_m \sin \theta, \quad (11)$$

where q_e and q_m are the electric and magnetic charges, respectively, while the subindex F means derivative with respect to F . Adopting the definitions

$$f_e = 2F_{01} F^{10} = 2q_e^2 L_F^{-2} r^{-4} \geq 0, \quad f_m = 2F_{23} F^{23} = 2q_m^2 r^{-4} \geq 0 \quad (12)$$

$F = f_m - f_e$ and the energy-momentum tensor can be written as

$$T_\nu^\mu = \frac{1}{2} \text{diag}(L + 2f_e L_F, L + 2f_e L_F, L - 2f_m L_F, L - 2f_m L_F), \quad (13)$$

The nonlinearity of the electromagnetic field modifies light trajectories that regularly are the null geodesics of the background metric $g_{\mu\nu}$. In nonlinear electromagnetism, instead, photons do propagate along null geodesics of an effective geometry with metric tensor $\gamma_{\text{eff}}^{\mu\nu}$ that depends on the nonlinear theory. The discontinuities of the electromagnetic field propagate obeying the equation for the characteristic surfaces. Then the effective metric can be

derived from the analysis of the characteristic surfaces [7] [8] . The corresponding equation for the gradient of the characteristic surfaces $S_{,\mu}$ is

$$(L_F g^{\mu\nu} - 4L_{FF} F_\alpha^\mu F^{\alpha\nu}) S_{,\mu} S_{,\nu} = \gamma_{\text{eff}}^{\mu\nu} S_{,\mu} S_{,\nu} = 0. \quad (14)$$

Calculating the metric components $\gamma_{\text{eff}}^{\mu\nu}$ the effective metric of the SSS spacetime is given by

$$ds_{\text{eff}}^2 = (L_F G_m)^{-1} \left\{ G_m G_e^{-1} \left(f(r) dt^2 - \frac{1}{f(r)} dr^2 \right) - r^2 d\Omega^2 \right\}. \quad (15)$$

G_m and G_e , the magnetic and electric factors that make the difference between the linear and nonlinear electromagnetism, are given by

$$G_m = \left(1 + 4L_{FF} \frac{q_m^2}{L_F r^4} \right), \quad G_e = \left(1 - 4L_{FF} \frac{q_e^2}{L_F^3 r^4} \right); \quad (16)$$

and in the linear limit become equal to one. In determining null geodesics conformal factors can be ignored, since they do not modify the null geodesics. Considering the geodesic motion in the equatorial plane of the effective spacetime (15), not including the conformal factor $(L_F G_m)^{-1}$, the corresponding effective potential V_r is

$$V_r = G_m^{-1} G_e \left[G_m^{-1} G_e E^2 - \frac{f(r) L^2}{r^2} \right]. \quad (17)$$

When we apply the first conditions for the (unstable) null circular orbits $V(r_c) = 0$, we obtain

$$\frac{E^2}{L^2} = \left(\frac{G_m}{G_e} \right)_{r_c} \frac{f_c}{r_c^2} \quad (18)$$

and jointly with the second condition, $V'(r_c) = 0$, the radius r_c of the circular null orbit is given by one of the roots of the following equation,

$$\left(\frac{G_e}{G_m} \right) \left(\frac{f'_c}{f_c} - \frac{2}{r_c} \right) - \left(\frac{G_e}{G_m} \right)'_{r_c} = 0. \quad (19)$$

Such root should be greater than the horizon radius, $r_c > r_h$; subscript ‘‘c’’ means that the quantity in question is evaluated at the radius $r = r_c$. This radius is also known as the radius of the photosphere, and defines the sphere of unstable circular photon trajectories.

The Lyapunov exponent (2) for the effective metric takes the form;

$$\lambda^2 = \frac{f_c r_c^2}{2} \left[\frac{f_c G_m}{r_c^2 G_e} \left(\frac{G_e}{G_m} \right)_c'' - \left(\frac{f}{r^2} \right)_c'' \right] \quad (20)$$

while the angular velocity (3) changes to

$$\Omega_c = \sqrt{\frac{G_m f_c}{G_e r_c^2}}. \quad (21)$$

Equations (20) and (21), the nonlinear electromagnetic version of (7) and (8), determine the quasinormal frequencies, imaginary and real parts, respectively, for NLEM black holes in the eikonal approximation.

From the expressions (16) and having determined the sign of L_{FF}/L_F it can be defined if G_m and G_e are greater or less than one. From that knowledge and the expression of Ω_c we can assert if the real part of the QNF is enhanced or suppressed as compared to the linear counterpart. For instance if $L_{FF}/L_F < 0$ then $G_m \leq 1$ and $G_e > 1$ and consequently, from (21), Ω_c gets a smaller value, resulting in a suppression of the real part of QNF ω_r .

The analysis is not so straightforward for the imaginary part, eq. (20), since it is not obvious which the sign of the second derivative of G_e/G_m will be. In this case we need more specific information about the NLEM lagrangian.

In the next section examples of different NLEM black holes are given and the QNF due to the NLEM field are compared with those corresponding to massless test particles as well as with the QNF originated from the linear electromagnetic black hole, the SSS solution to the Einstein-Maxwell equations, the Reissner-Nordstrom.

IV. EXAMPLES

We calculate the QNFs of four SSS black hole solutions corresponding to different NLEM theories coupled to gravity. First will be addressed two examples of singular NLEM black holes, the Born-Infeld (BI) and a magnetic solution for the Euler-Heisenberg electrodynamics coupled to gravity. Then we analyse the QNM response of two regular NLEM black holes: the Bardeen magnetic monopole and one Bronnikov solution, comparison with massless particles and linear electromagnetism is established as well. It is considered only the fundamental frequency $n = 0$, that is the least damped mode.

A. The QNM of the Reissner-Nordstrom black hole

The RN is the SSS solution to the action (10) with $L = F$, $L_F = 1$ and $L_{FF} = 0$ and then the nonlinear factors are $G_e = 1$ and $G_m = 1$. For each example addressed in what follows RN will be the reference to analyze the QNFs behavior. Briefly the RN case is exposed.

In the eikonal or geometric-optics limit, the QNFs are given by (1) with λ and Ω_c calculated as in (7) and (8), respectively. For the RN black hole, the metric function in the line element (4) is given by

$$f(r) = g(r) = 1 - \frac{2M}{r} + \frac{Q^2}{r^2}, \quad (22)$$

while the circular null orbit radius r_c is calculated from (9), that in the RN case amount to the quadratic polynomial

$$r_c^2 - 3Mr_c + 2Q^2 = 0, \quad r_c = \frac{1}{2}(3 + \sqrt{9 - 8Q^2}). \quad (23)$$

where we have used a dimensionless coordinate $r \rightarrow r/M$ and $Q \rightarrow Q/M$. The functions λ and Ω_c are given by (7) and (8),

$$\lambda^2 = \frac{1}{r_c^6}(r_c^2 - 2Q^2)(Q^2 + r_c^2 - 2r_c), \quad \Omega_c^2 = \frac{1}{r_c^4}(r_c^2 - 2r_c + Q^2), \quad (24)$$

that substituting r_c from (23) give

$$\lambda^2 = \frac{16\sqrt{9 - 8Q^2}(3 - 2Q^2 + \sqrt{9 - 8Q^2})}{(3 + \sqrt{9 - 8Q^2})^5}, \quad \Omega_c^2 = \frac{8(3 - 2Q^2 + \sqrt{9 - 8Q^2})}{(3 + \sqrt{9 - 8Q^2})^4}. \quad (25)$$

These are the expressions that we will use in the comparisons with the NLEM cases. In the RN case analytic solutions can be found all the way through. In none of the NLEM examples presented analytic solutions were determined. Recent works on aspects of RN-QNM are [12] [13].

B. Born-Infeld black hole

The BI nonlinear electrodynamics was first considered by Born and Infeld in an attempt to cure at the classical level the singularity of the electric field of a point charge [6]. Born-Infeld electrodynamics possesses several interesting physical features like the absence of

birrefringence, the Maxwell limit for weak electromagnetic field, as well as the finiteness of the electric field at the charge position. The Einstein–Born–Infeld (EBI) generalization of the Reissner Nordström (RN) black hole was obtained by García, Salazar and Plebański in [14]; the geodesic structure of BI black hole was studied in [15] and recently in [16]. This Einstein–Born–Infeld solution is singular at the origin and it is characterized by three parameters: mass, charge and the BI parameter; the BI black hole can present one, two or none horizons depending on the values of the parameters. The Born–Infeld Lagrangian is given by

$$(L(F) = 4b^2 \left(-1 + \sqrt{1 + \frac{F}{2b^2}} \right). \quad (26)$$

For a line element of the form (4) the solution to the EBI equations is given by the metric function

$$f(r) = g(r) = 1 - \frac{2M}{r} + \frac{2}{3}r^2b^2 \left(1 - \sqrt{1 + \frac{q^2}{b^2r^4}} \right) + \frac{2}{3} \frac{q^2}{r} \sqrt{\frac{b}{q}} \mathbb{F} \left(\arccos \left[\frac{br^2/q - 1}{br^2/q + 1} \right], \frac{1}{\sqrt{2}} \right), \quad (27)$$

where \mathbb{F} is the elliptic integral of the first kind, M is the mass parameter, q is the electric charge (both in length units) and b is the Born-Infeld parameter that corresponds to the magnitude of the electric field at $r = 0$. The nonvanishing component of the electromagnetic field is $F_{rt} = q \left(r^4 + \frac{q^2}{b^2} \right)^{-1/2}$. The nonlinear factors G_m and G_e are, in case that we are considering only electric charge, $q_m = 0$,

$$G_m = 1, \quad G_e = \left(1 + \frac{q^2}{b^2r^4} \right). \quad (28)$$

Hereafter we consider $\omega_r \mapsto \omega_r/l$ for our analysis [9]. In Fig. 1 it is shown the behavior of the QNFs ω_i and ω_r of the BI black hole for two different values of the parameter b and are compared with RN black hole. The imaginary part of QNF ω_i , for RN case, increases as q augments and presents a maximum then decreasing; for RN the value of q cannot exceed $q = 1$ that corresponds to the extreme black hole, $q = M$. BI does not have this constraint, and ω_i increases without bound for small values of b . Therefore BI- ω_i is enhanced as compared with RN. The opposite occurs with the BI- ω_r that is suppressed as compared with RN. Both frequencies approach the RN limit as b increases.

The QNF coming from massless particles and photons (ph) are compared in Fig. 2. For the imaginary part, ω_i , the previous behavior is enhanced even more in photon trajectories,

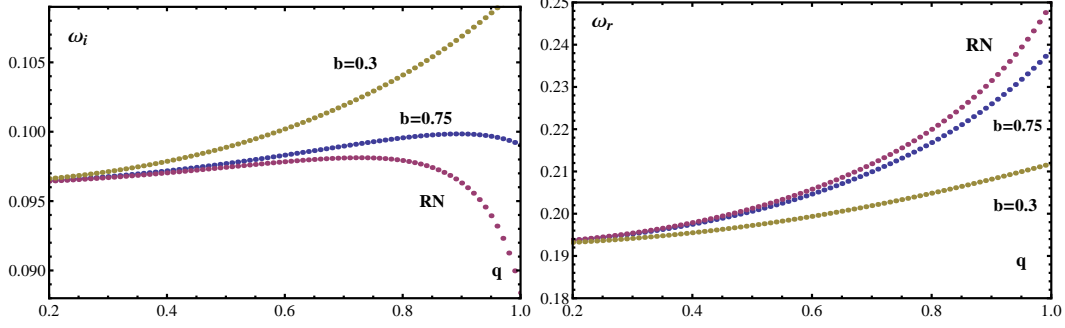


FIG. 1: The behavior of ω_i and ω_r For the BI and RN black holes is shown as functions of the charge. Two values of b were considered, $b = 0.3$ and $b = 0.75$; the other parameters fixed: $M = 1$ and $n = 0$.

while ω_r -massless particles values are greater than photon's. Massless test particles QNFs were analyzed in [10] using the WKB approximation.

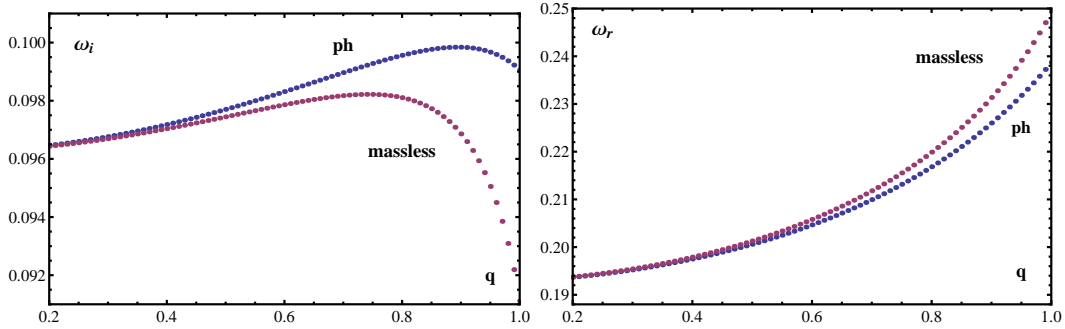


FIG. 2: Comparison between ω_i and ω_r of the BI black hole for massless particles and photon (ph) trajectories is shown. The rest of parameters are $M = 1$, $b = 0.75$ and $n = 0$.

C. Euler-Heisenberg Black hole

The effective action for electrodynamics due to one-loop quantum corrections was calculated by Euler and Heisenberg (EH). For the low-frequency limit $\omega \ll m_e c^2 / \hbar$ the effective Lagrangian with magnetic charge [17] takes the form

$$L(F) = F(1 - aF) \quad (29)$$

with $a = \hbar e^2 / (360\pi^2 m_e^2)$, where \hbar , e , and m_e are the Planck constant, electron charge, and electron mass, respectively. BI theory applies for fields even stronger than the ones in QED, because it turns out that a Lagrangian very similar to (29) can be obtained in the “weak” field limit of the BI Lagrangian: expanding the square root in (26) up to second order, $(1+x)^{1/2} = 1 + x/2 - x^2/8 + \dots$, we obtain

$$L(F) = 4b^2 \left(-1 + 1 + \frac{F}{4b^2} + \frac{F^2}{32b^4} + \dots \right) = F - \frac{F^2}{8b^2}, \quad (30)$$

from the comparison with (29) a relationship between the EH and BI parameters is obtained, $8b^2 = a^{-1}$. For the previous reasons we expect for the EH-QNFs a very similar behavior than the BI frequencies. Indeed this is the case.

In [17] a solution of the EH field coupled to gravity equations was found (see also [18]). It corresponds to a SSS magnetic black hole with metric elements in (4) given by

$$f(r) = g(r) = 1 - \frac{2M}{r} + \frac{q^2}{r^2} - \frac{2}{5}a\frac{q^4}{r^6} \quad (31)$$

where M is the mass parameter, $q = q_m$ is the magnetic charge. One or two horizons may occur: if $(M/q)^2 \leq 24/25$ a single horizon exists but for $(M/q)^2 > 24/25$ a second and a third horizons occur. Extremal solutions exist only for $a^2 \leq a_{crit}^2 = (8/27)q^2$. The electromagnetic invariant is $F = 2q^2/r^4$. Since $q_e = 0$, the G_e and G_m factors are

$$G_e = 1, \quad G_m = \left(1 + \frac{8aq^2}{4aq^2 - r_c^4} \right) \quad (32)$$

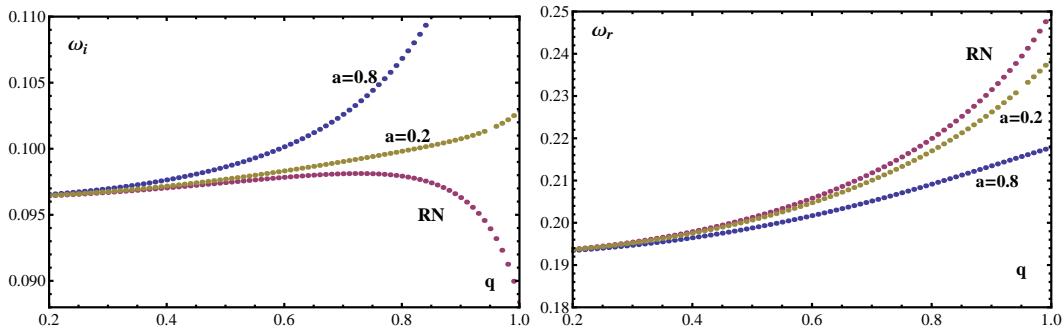


FIG. 3: The behavior of ω_i and ω_r in terms of the charge q is shown for the EH and RN black holes; the rest of parameters fixed as $M = 1$ and $n = 0$

The behavior of QNFs ω_i and ω_r for EH black hole resembles the BI ones (see Fig. 3), taking into account that the nonlinear parameters b and a are inversely proportional, for small a 's we obtain an effect similar to large b 's, i.e. the behavior approaches the RN one. While for larger a 's the departure from RN behavior is clear, enhanced for ω_i and suppressed for ω_r . Regarding the massless-photon comparison, ω_i is enhanced and ω_r is suppressed for photons respect to massless particle trajectories as can be seen in Fig.4.

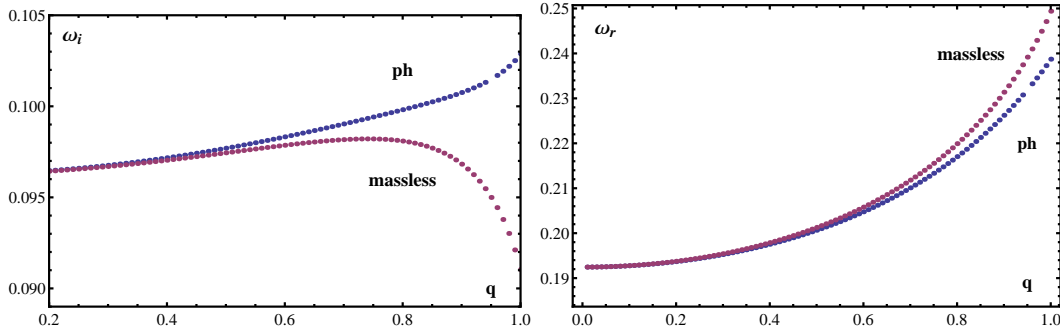


FIG. 4: Comparison for varying charge of photon vs. massless particle QNFs, imaginary and real parts, ω_i and ω_r , for the EH black hole. In this plot $M = 1$, $a = 0.2$ and $n = 0$

D. Bardeen black hole

This model was proposed by Bardeen in the sixties as an example of a regular black hole; later on Ayón-Beato and García [19] found a nonlinear electromagnetic source for such a black hole. Hence, the Bardeen black hole can be interpreted as a self-gravitating nonlinear magnetic monopole with mass M and charge $q_m = g$, derived from Einstein gravity coupled to the Lagrangian

$$L(F) = \frac{6}{sg^2} \frac{(g^2 F/2)^{\frac{5}{4}}}{(1 + \sqrt{g^2 F/2})^{\frac{5}{2}}} \quad (33)$$

where $s = |g|/2M$. A solution for the coupled Einstein-Bardeen Lagrangian for a static spherically symmetric space has the metric function $f(r) = g(r)$ given by

$$f(r) = 1 - \frac{2Mr^2}{(r^2 + g^2)^{\frac{3}{2}}}, \quad (34)$$

The solution (34) presents horizons only if $2s = g/m \leq 0.7698$. The electromagnetic invariant is $F = 2g^2/r^4$ and the G_e and G_m factors are given by

$$G_e = 1, \quad G_m = 1 - \frac{4(6g^2 - r^2)}{8(r^2 + g^2)}. \quad (35)$$

The radius of the unstable circular orbit r_c is found numerically from (19) and care must be taken in that such root be greater than the horizon radius, $r_c > r_h$.

The behavior of the QNMs from light rays impinging upon Bardeen black hole are shown in Fig.5. ω_i decreases when g increases and similarly for massless particles and photons. This behavior is in contrast with the two previously analyzed examples; the resemblance with RN ω_i occurs only when the charge approaches zero. Regarding ω_r the behavior for massless particles is indistinguishable from RN one. The one corresponding to photons is odd in the sense that not even in the limit that charge goes to zero the RN behavior is recovered; one possible explanation may be the nature of the solution because charge and mass parameters are not independent, and in fact when charge is turned off, so does the mass whose origin is purely electromagnetic. QNFs for massless particles have been determined in [9].

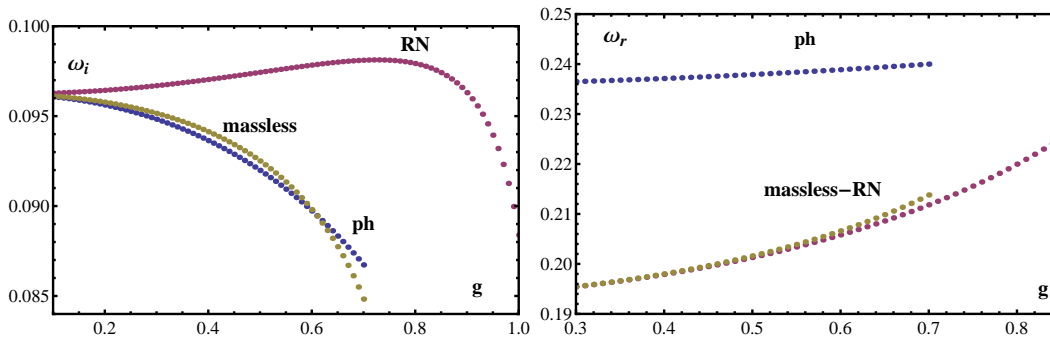


FIG. 5: It is shown the behavior of ω_i and ω_r of the Bardeen black hole as functions of the charge g , keeping fixed $M = 1$ and $n = 0$.

E. Bronnikov magnetic black hole

In [20] NLEM Lagrangians coupled to gravity were analyzed focusing on the properties that lead to nontrivial regular metrics. No go theorems forbid regular electric black holes, but magnetic ones can be found. One example is the presented in the same reference, with the Lagrangian

$$L(F) = F \operatorname{sech}^2[a(F/2)^{1/4}] \quad (36)$$

where a is a constant. The metric function in the line element of the form (4) is

$$f(r) = 1 - \frac{g^{3/2}}{ar} \left[1 - \tanh\left(\frac{a\sqrt{g}}{r}\right) \right] \quad (37)$$

the constant a is related to the mass m and the magnetic charge g by $a = g^{3/2}/(2M)$. The solution corresponds to a black hole if $M/g > 0.96$. The electromagnetic invariant is $F = 2g^2/r^4$. For a purely magnetic charge $G_e = 1$ and

$$G_m = \frac{g^2 \sinh^2(\frac{g^2}{2Mr}) \left(-2g^2 + g^2 \cosh(\frac{g^2}{2Mr}) - 5Mr \sinh(\frac{g^2}{2Mr}) \right)}{4Mr \left(-4Mr^3 + g^2 \tanh(\frac{g^2}{2Mr}) \right)} \quad (38)$$

The QNFs behavior when the charge is varying is shown in Fig. 6. The imaginary part of QNF ω_i for massless particles as well as for photon reproduces the RN one, and slight departure is observed only when the charge approaches its upper limit. As for the real QNF, ω_r , for massless particles is coincident with RN for any charge, while small difference occurs for photons. From all of the examined examples Bronnikov black hole is the one in which the nonlinear effects are the least.

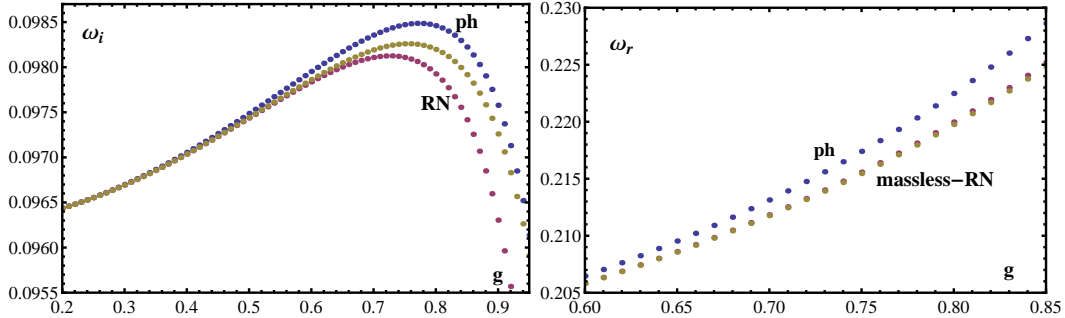


FIG. 6: QNFs ω_i and ω_r of the Bronnikov black hole are shown as functions of the charge g ; the other parameters fixed to $M = 1$ and $n = 0$.

V. CONCLUSIONS

We have studied the QNM frequencies of NLEM black holes through Lyapunov exponent in the optical approximation. QNFs were calculated from the unstable null geodesics of

the effective metric. Effective metric is obtained from the regular metric but taking into account the NLEM effects. From the expressions of the real and imaginary parts of the QNFs and Eqs. (20) and (21), it is clear that the NLEM effects will modify QNF enhancing or suppressing them, depending on the sign of the quotients L_{FF}/L_F and of the second derivative of G_e/G_m . The NLEM effects manifest on the dynamics of the light perturbations modifying the oscillation periods as well as the damping times.

The obtained QNFs, in the eikonal approximation, are calculated to four SSS black hole solutions corresponding to different NLEM theories coupled to gravity. In all cases comparison is done with the QNFs of the linear counterpart, the RN black hole. In three of the examples (BI, EH and Bronnikov solution), the NLEM effect when the charge is varied consists in suppressing the real part while increasing the imaginary one, i.e. oscillation periods are larger and relaxation occurs faster.

Comment apart deserves the Bardeen black hole. In this case the effect is the opposite: the real QNF is enhanced while the imaginary part is suppressed; notoriously the real frequency is not recovered when the charge approaches zero. Several explanations come to mind, among them is that mass and charge parameters are not independent in this solution and the limit to zero of the charge cannot be taken separately from the value of the mass, since the origin of the mass is magnetic; this is a self-gravitating magnetic structure. Additionally, the comparison between the behavior of massless particles and photons was done.

A thorough analysis is needed to know how the modifications introduced by NLEM effects influence the black hole stability. Another point of interest would be checking if there is any consequence of introducing NLEM related to the conjectured relationship between the real part of the QNF and the black hole area quantization.

Acknowledgments

N. B. acknowledges partial support of CONACyT (Mexico), project 166581

-
- [1] B. P. Abbott et al. Observation of Gravitational Waves from a Binary Black Hole Merger. *Phys. Rev. Lett.*, 116(6):061102, 2016.

- [2] Gabor Kunstatter. d-dimensional black hole entropy spectrum from quasinormal modes. *Phys. Rev. Lett.*, 90:161301, 2003.
- [3] Bahram Mashhoon. Stability of charged rotating black holes in the eikonal approximation. *Phys. Rev.*, D31(2):290–293, 1985.
- [4] Valeria Ferrari and Bahram Mashhoon. New approach to the quasinormal modes of a black hole. *Phys. Rev.*, D30:295–304, 1984.
- [5] Vitor Cardoso, Alex S. Miranda, Emanuele Berti, Helvi Witek, and Vilson T. Zanchin. Geodesic stability, Lyapunov exponents and quasinormal modes. *Phys. Rev.*, D79:064016, 2009.
- [6] M. Born and L. Infeld. Foundations of the new field theory. *Proc. Roy. Soc. Lond.*, A144:425–451, 1934.
- [7] M. Novello, V. A. De Lorenci, J. M. Salim, and Renato Klippert. Geometrical aspects of light propagation in nonlinear electrodynamics. *Phys. Rev.*, D61:045001, 2000.
- [8] S. A. Gutierrez, A. L. Dudley, and J. F. Plebanski. Signals and Discontinuities in General Relativistic Nonlinear Electrodynamics. *J. Math. Phys.*, 22:2835–2848, 1981.
- [9] Sharmanthie Fernando and Juan Correa. Quasinormal Modes of Bardeen Black Hole: Scalar Perturbations. *Phys. Rev.*, D86:064039, 2012.
- [10] Sharmanthie Fernando. Gravitational perturbation and quasi-normal modes of charged black holes in Einstein-Born-Infeld gravity. *Gen. Rel. Grav.*, 37:585–604, 2005.
- [11] Jin Li, Kai Lin, and Nan Yang. Nonlinear electromagnetic quasinormal modes and Hawking radiation of a regular black hole with magnetic charge. *Eur. Phys. J.*, C75(3):131, 2015.
- [12] Mauricio Richartz and Davi Giugno. Quasinormal modes of charged fields around a Reissner-Nordström black hole. *Phys. Rev.*, D90(12):124011, 2014.
- [13] Christian Corda, Seyed Hossein Hendi, Reza Katebi, and Nathan O. Schmidt. Hawking radiation - quasi-normal modes correspondence and effective states for non-extremal Reissner-Nordstrom black holes. *Adv. High Energy Phys.*, 2014:527874, 2014.
- [14] A. García D., H. Salazar I., and J. F. Plebański. Type-d solutions of the einstein and born-infeld nonlinear-electrodynamics equations. *Il Nuovo Cimento B (1971-1996)*, 84(1):65–90, 1984.
- [15] N. Breton. Geodesic structure of the Born-Infeld black hole. *Class. Quant. Grav.*, 19:601–612, 2002.

- [16] Romn Linares, Marco Maceda, and Daniel Martnez-Carbajal. Test Particle Motion in the Born-Infeld Black Hole. *Phys. Rev.*, D92(2):024052, 2015.
- [17] Hiroki Yajima and Takashi Tamaki. Black hole solutions in Euler-Heisenberg theory. *Phys. Rev.*, D63:064007, 2001.
- [18] V. A. De Lorenci, N. Figueiredo, H. H. Fliche, and M. Novello. Dyadosphere bending of light. *Astron. Astrophys.*, 369:690, 2001.
- [19] Eloy Ayon-Beato and Alberto Garcia. The Bardeen model as a nonlinear magnetic monopole. *Phys. Lett.*, B493:149–152, 2000.
- [20] Kirill A. Bronnikov. Regular magnetic black holes and monopoles from nonlinear electrodynamics. *Phys. Rev.*, D63:044005, 2001.